

## Model for reversal dynamics of ultrathin ferromagnetic films

I. Ruiz-Feal, T. A. Moore, L. Lopez-Diaz, and J. A. C. Bland  
*Cavendish Laboratory, University of Cambridge, Cambridge CB3 0HE, United Kingdom*  
 (Received 20 July 2001; published 8 January 2002)

We propose a phenomenological model for the dynamic magnetization reversal of epitaxial ultrathin ferromagnetic films with uniaxial in-plane anisotropy. The model assumes that the reversal proceeds via the nucleation of small reversed domains and subsequent domain wall propagation, and that the domain wall velocity depends linearly on the applied magnetic field strength. Two regimes in the dynamic coercive field ( $H_c^*$ ) versus applied field sweep rate [ $\ln(\Delta H/\Delta t)$ ] data are found in good agreement with experiments. For ultrathin films, the mobility of the domain wall ( $\mu$ ) is found to vary with the thickness of the film ( $t$ ) according to a power law.

DOI: 10.1103/PhysRevB.65.054409

PACS number(s): 75.40.Gb, 75.40.Mg, 75.70.Rf

### I. INTRODUCTION

The dynamics of magnetization reversal in ultrathin ferromagnetic films is currently being extensively studied from both a fundamental and applied standpoint. Key questions concern the physical processes involved in domain nucleation, domain wall motion, their link to coercive field, influence of crystallographic structure, etc. During the last few years, the significance of the field sweep rate for the dynamics of magnetization reversal in epitaxial thin films has been studied.<sup>1-7</sup> In these studies, the coercive field of ferromagnetic epitaxial ultrathin films was monitored as a function of the sweep rate of an oscillating applied magnetic field and the coercivity was found to increase with sweep rate. Recently, it has been found that the dynamic coercivity ( $H_c^*$ ) varies with applied field sweep rate ( $\dot{H}$ ) as  $H_c^* \sim \dot{H}^\alpha$ , but that two regimes are obtained: at low and high frequency different values of  $\alpha$  are found. This important finding appears to be a general feature of ultrathin ferromagnetic films.<sup>2,3,8</sup>

Different models have been proposed aiming at understanding this phenomenon. Sharrock *et al.* considered the statistical thermodynamic behavior of multiple isolated particles<sup>9</sup> which can be applied to polycrystalline thin films. Raquet *et al.* developed a model for epitaxial films in which the experimental reversal behavior was attributed to a competition between the relative importance of domain nucleation and domain wall propagation effects.<sup>2</sup> The conclusions of Raquet *et al.* suggested that domain wall motion in Au/Co/Au sandwiches was the main mechanism in the reversal process for low sweep rates, whereas domain nucleation dominated at high sweep rates. A difficulty which arises from this analysis is that different values of the wall velocity and nucleation rate are assumed for high and low sweep rates.

In this work we propose an alternative simple model for the dynamic reversal mechanism in epitaxial ultrathin films. Domain nucleation rate and domain wall propagation effects will be considered in order to understand the observed change of coercive field as a function of sweep rate. In this model, only two parameters will be shown to be necessary to describe the process, and these parameters are independent of any external factor (e.g., applied field sweep rate).

### II. MOTIVATION

In experiments reported in Refs. 2, and 3 and 8, epitaxial Fe/GaAs and Au/Co/Au magnetic films were reversed via an alternating magnetic field. It was shown that the coercive field of the films increases with the applied field sweep rate. In this paper we will work on Fe/GaAs(001) magnetic films.

A typical result is shown in Fig. 1(a). It shows the dependence of the dynamic coercive field ( $H_c^*$ ) on the sweep rate for a 55-Å Fe/GaAs(001) epitaxial film. The sample preparation and experimental conditions are given in detail elsewhere.<sup>3</sup> In the low dynamic regime [ $\ln(\Delta H/\Delta t) < 0$ ],  $\ln(H_c^*)$  is approximately linearly dependent on  $\ln(\Delta H/\Delta t)$ . At higher sweep rates,  $\ln(H_c^*)$  increases at a larger rate. (In this paper, all logarithms will be decimal unless otherwise stated.)

In a further recent study, it has been found that the slope ( $\alpha$ ) of the linear fit of  $\ln(H_c^*)$  vs  $\ln(\Delta H/\Delta t)$  in epitaxial Fe/GaAs(001) samples varies with thickness for low sweep rates as shown in Fig. 1(b). Similar results on Au/Co/Au sandwiches have found by other authors.<sup>10</sup>

This paper aims at understanding these experimental data from a phenomenological standpoint. On the one hand, we intend to understand why the coercivity of the magnetic film and applied field sweep rate are linked via the power law  $H_c^* \sim \dot{H}^\alpha$ , and why there are two distinct dynamic regimes. On the other hand, we intend to understand why the slope ( $\alpha$ ) in the low dynamic regime increases as the thickness of the film decreases.

### III. DESCRIPTION OF THE MODEL

It has been experimentally seen that the dependence of domain wall velocity on applied field strength for an in-plane magnetized ultrathin epitaxial Ag/Fe/Ag(001) film follows a linear response characteristic of a viscous damping movement.<sup>11</sup> This response follows the equation

$$v(h) = \begin{cases} 0, & |h| < h_{dp}, \\ \mu(|h| - h_{dp}), & |h| \geq h_{dp}, \end{cases} \quad (1)$$

where  $\mu$  is the domain wall mobility, a phenomenological parameter characteristic of the magnetocrystallographic

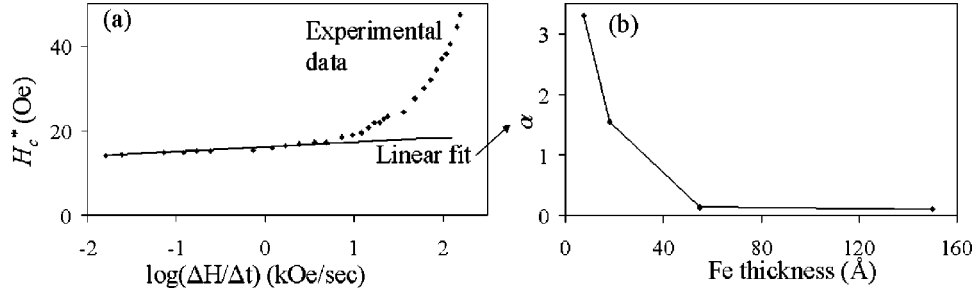


FIG. 1. (a) Experimental dynamic coercive field ( $H_c^*$ ) vs  $\ln(\Delta H/\Delta t)$  of applied magnetic field (dots) (Ref. 3) and linear fit to the low dynamic regime. (b) Slope of linear fits ( $\alpha$ ) as a function of Fe thickness in Fe/GaAs(001) films.

properties of the film and growth conditions, and  $h_{dp}$  is the depinning field, the field at which the domain wall is depinned and sweeps the magnetic film.

We will assume that a density  $\rho$  of reversed domains are present at the depinning field. Given such a system with reversed domains, the domain walls will expand at a velocity described by Eq. (1). The average area ( $A$ ) that a domain wall will have to cover to complete the reversal will be

$$A = \frac{1}{\rho}. \quad (2)$$

Three approaches will be considered: in the simplest one we will assume that the domain walls are straight (model 1). In the second one, a more realistic picture will be considered by assuming that the domain walls are circular (model 2). This assumption is based on magnetic images of reversal processes shown in Ref. 12. In these two models, the number of reversed domains nucleated is considered to be constant throughout the process. A further refinement will be introduced by assuming that the density of reversed domains will depend on the applied magnetic field (model 3). Figure 2 illustrates these models schematically. In each case, domain walls are considered to be noninteracting and evenly distributed.

### A. Straight domain wall

In model 1, each domain wall is considered to be a straight line. Regardless of the actual size of the magnetic sample, given a density  $\rho$  of domain walls, the average area that each one of them will have to sweep to complete the reversal will be  $A = 1/\rho$ . For simplicity, we will consider that each domain will have to sweep a square of lateral size  $\sqrt{A}$  (that is, we have divided the magnetic sample in small cells

of area  $A$ , each one of them corresponding to a single domain wall). During the reversal process, the change of the normalized magnetization ( $m$ ) with time will be

$$dm(t) = \pm 2 \frac{\sqrt{A} v(h(t)) dt}{A}. \quad (3)$$

The “+” sign is taken for  $h > 0$  and the “-” for  $h < 0$ . Considering Eqs. (1), (2), and (3),

$$dm(t) = \pm \sqrt{\rho} \mu [h(t) - h_{dp}] dt. \quad (4)$$

In further sections, the importance of the parameter  $\mathcal{T} = \sqrt{\rho} \mu$  in this model will be discussed. Briefly, it should be noted that the speed of the dynamics of the process scales to  $\mathcal{T}$ . This parameter will play an important role in the susceptibility of the film to external changes, since the lower it is, the more time the film will spend in the reversal process.

Following Eq. (4), a hysteresis loop will be computed applying a sinusoidal field

$$h(t) = H_0 \sin(2\pi\Omega t). \quad (5)$$

The sample will be considered to be initially saturated at a negative value ( $m = -1$ ). Then, at the depinning field ( $h_{dp}$ ), the density  $\rho$  of reversed domains present in the sample will propagate with a velocity described by Eq. (1). If the system completes reversal, an analogous process will happen backwards at negative fields. On the contrary, if the frequency of the applied field is too high and the domain wall does not have enough time to complete reversal, it will stop halfway through following equation (1) and will start moving backwards at negative applied field. The results of hysteresis loop calculations, for different frequencies, can be seen in Fig. 3 (left column). It can be seen that in the cases in which saturation is reached,  $H_c^*$  increases as the frequency of the mag-

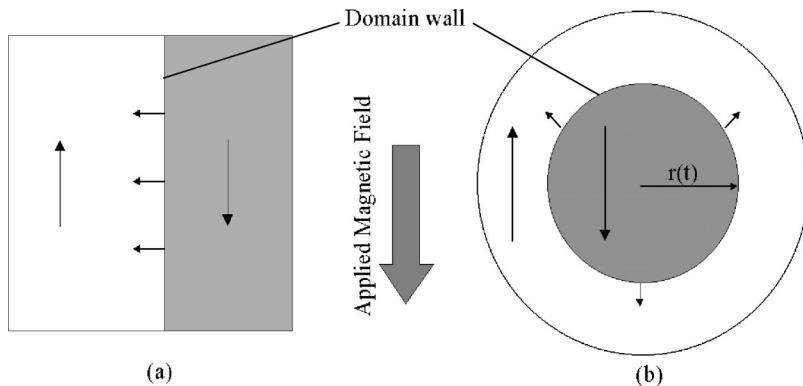


FIG. 2. Sketch of the physical pictures proposed. (a): Straight domain wall (model 1). (b): Circular domain wall (models 2 and 3).

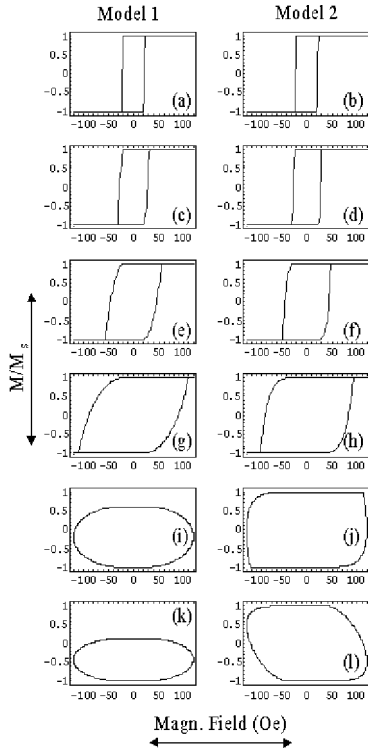


FIG. 3. Hysteresis loops using models 1 (left column) and 2 (right column), for frequencies  $\Omega=10^3$  (a),(b),  $10^4$  (c),(d),  $10^5$  (e),(f),  $7.94 \times 10^5$  (g),(h),  $3.55 \times 10^6$  (i),(j), and  $5.01 \times 10^6$  (k),(l)  $s^{-1}$ , keeping the other parameters constant:  $H_0=120$  Oe,  $h_{dp}=20$  Oe,  $\mu=100$  (m/s)/Oe, and  $\rho=10^6$   $m^{-2}$ .

netic field increases. Further details of the computing procedure are explained in the Appendix.

### B. Circular domain wall

A modified version of the model, which may be more realistic for ultrathin Fe films, was introduced (model 2). According to scanning Kerr microscopy images of reversal processes shown by Cowburn *et al.*<sup>12</sup> [Fig. 5], a better approach would be to consider circular walls rather than straight ones [Fig. 2(b)]. This was implemented in the computations by introducing a new evolution equation for the magnetization during reversal:

$$dm(t) = \pm 2 \frac{2\pi r(t) dr(t)}{A}, \quad (6)$$

where  $r(t)$ , the radius of a circular domain wall, will expand or shrink during reversal linearly with time as  $dr(t) = v(t)dt$ . Considering Eqs. (1), (2), and (6),

$$dm(t) = \pm 4\pi\rho\mu^2 \int_{t_0}^t [ |h(t')| - h_{dp} ] dt' [ |h(t)| - h_{dp} ] dt, \quad (7)$$

where  $t_0$  is the moment at which  $h(t_0) = h_{dp}$ . In this new model, the magnetization  $[m(t) = m_{t=0} + \int_{t_0}^t dm(t')]$  evolves with  $t^2$ , whereas this relation was linear in the previous

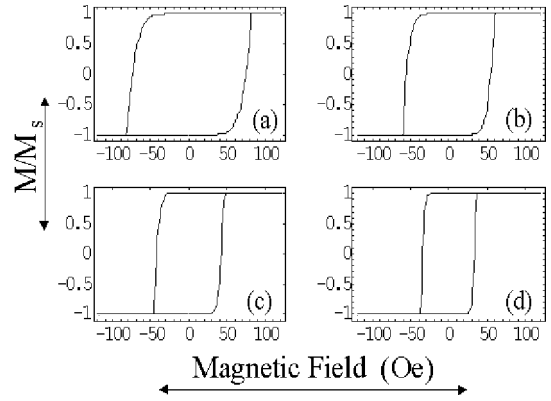


FIG. 4. Hysteresis loops calculated with model 3 for  $\eta=10^4$  (a),  $10^5$  (b),  $10^6$  (c), and  $10^7$  (d)  $m^{-2}$  Oe $^{-1}$ ,  $H_0=120$  Oe,  $h_{dp}=20$  Oe,  $\Omega=10^{5.5}$   $s^{-1}$ , and  $\mu=100$  (m/s)/Oe.

model. In this case, the quantity that governs the scaling of the reversal time is  $\tilde{T}^2 = \rho \mu^2$ , instead of  $T$  as in model 1.

Figure 3 (right column) shows typical hysteresis loops calculated with this model for different values of the frequency  $\Omega$ . In this new case of a circular domain wall, at the beginning of the reversal the system evolves at a lower speed compared to a straight wall, but as the radius of the circular domain wall increases the reversal gets faster.

### C. Field-dependent nucleation

In models 1 and 2, it was considered that the density of domain walls was constant. In order to examine the importance of nucleation effects, a constant rate of nucleation  $[R(h) = \eta]$  of reversed domains for  $h > h_{dp}$  was implemented, as a first approximation, under the circular-wall picture:

$$\rho(h) = \begin{cases} 0, & h < h_{dp}, \\ \eta(|h| - h_{dp}), & h \geq h_{dp}. \end{cases} \quad (8)$$

More realistic models would include a field-dependent nucleation rate.<sup>2</sup> Strictly speaking,  $h_{dp}$  should differ between Eqs. (1) and (8) since nucleation and propagation effects are based on different physical phenomena. Nevertheless, they are related<sup>11</sup> and will be considered to be the same as a first approximation.

Figure 4 shows the dependence of hysteresis loops on different values of  $\eta$ . It can be seen that higher  $\eta$  (i.e., more nucleation) means a lower dynamic coercive field in this model. In this case,  $\tilde{T}^2 = \eta\mu^2$  is the quantity that governs the scaling of reversal time.

## IV. RESULTS AND DISCUSSION

### A. Dynamic coercivity

To understand the experimental data shown in Fig. 1(a), the dependence of coercive field on sweep rate was explored by computing hysteresis loops for various frequencies. A typical result is shown in Fig. 5. Good agreement with the experimental data is achieved. When the sweep rate is slow

enough, a quasilinear response of  $H_c^*$  is seen. At high sweep rates,  $H_c^*$  increases rapidly with  $\ln(\Delta H/\Delta t)$ , as observed in experiments.

In this model, when the sweep rate is slow enough, the domain walls sweep the film at almost constant magnetic field, showing a quasilinear dependence of  $H_c^*$  on  $\ln(\Delta H/\Delta t)$ . As the sweep rate increases, when the domain walls are nucleated and start to travel, the magnetic field has already reached higher values compared to those at low sweep rate, increasing rapidly the speed of the domain wall and decreasing the reversal time. Despite this decrease in reversal time with sweep rate, at high frequencies, the magnetic field strength at which  $m=0$  is higher than the one obtained for low sweep rates. Thus, the dynamic coercivity increases.

According to our model, the value of  $H_c^*$  at very low sweep rates is related to  $h_{dp}$  since, in this case, all the reversal will take place at almost the same field in which the reversal was actually launched,  $h_{dp}$ . That is,  $\lim_{\Omega \rightarrow 0} H_c^* = h_{dp}$ .

### B. Slope of quasilinear regime

The slope of the quasilinear regime is expected to be strongly related to the speed of the reversal (i.e., to  $\mathcal{T} = \sqrt{\rho} \mu$ ). The higher the speed of the reversal (i.e., the higher  $\mathcal{T}$ ), the less influence any external factor (such as  $\Omega$ ) will have on the system, since the domain walls will take less time to reverse the magnetization. The dependence of the slope of the quasilinear regime ( $\ln \Omega \leq 0$ ) on  $\mathcal{T}$  was monitored. Comparison of Fig. 6 (top) with Fig. 1(b) shows a strong correlation between  $\mathcal{T}$  and the thickness of the magnetic film ( $t$ ). A coordinate transformation  $\mathcal{T}' = a\mathcal{T}^b$  was implemented to relate  $\mathcal{T}$  to the thickness  $t$ . The values  $a = 1.75$  and  $b = 0.43$  were found to best fit experimental data of Fig. 1(b). Figure 6 (bottom) shows this fit. In this way, a link between the mobility ( $\mu$ ), the density of domain walls ( $\rho$ ), and the thickness ( $t$ ) of the magnetic films has been found for the set of samples reported in Ref. 8:

$$\mu \sqrt{\rho} = 0.27 t^{2.30}. \quad (9)$$

To our knowledge, this is the first time that a correlation between thickness, mobility, and domain wall density is obtained. This correlation suggests that the thinner the film, the

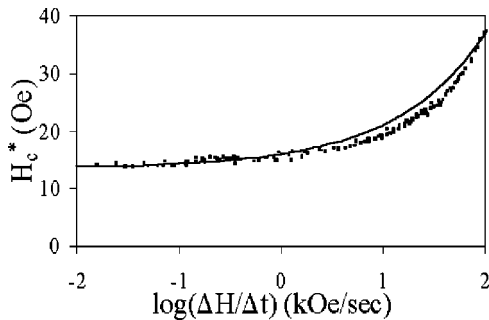


FIG. 5. Dots: experimental data (Ref. 3). Line: computational results, using model 1, of  $H_c^*$  vs  $\ln(\Delta H/\Delta t)$  (kOe/sec), for  $H_0 = 120$  Oe,  $h_{dp} = 14$  Oe,  $\mu = 0.9$  (m/s)/Oe; and  $\rho = 10^5$  m<sup>-2</sup>.

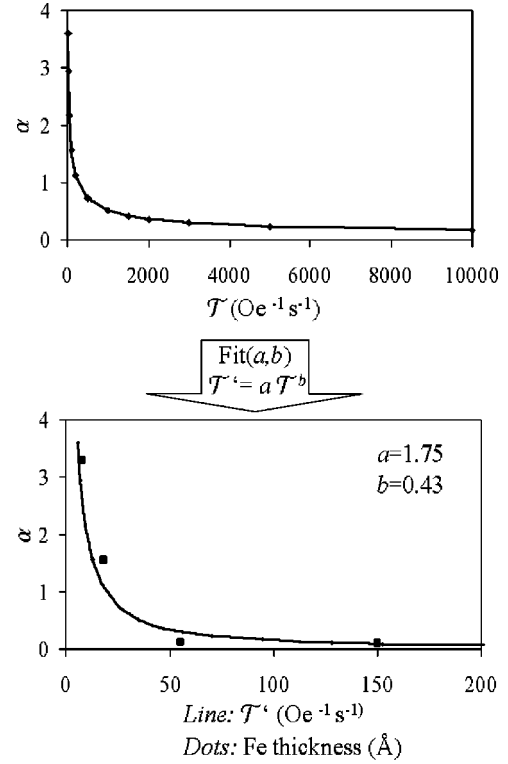


FIG. 6. Top: computed slope ( $\alpha$ ) of the quasi-linear regime vs  $\mathcal{T}$  using model 1. Bottom: Fit of the result on top to experimental data via a coordinate transformation  $\mathcal{T}' = a\mathcal{T}^b$ .

lower  $\sqrt{\rho}$  (i.e., the nucleation) and/or  $\mu$  (i.e., the domain wall mobility). We find it reasonable to think that the influence of defects due to interface roughness will be more significant for thinner films. Since those defects act as domain wall pinning sites, we should expect to see a reduced domain wall mobility as the thickness diminishes, as this model predicts.

### C. Reversal time

Regarding the reversal time, we have measured the reversal time of Fe/GaAs(001) and Fe/InAs(001) ultrathin films in which the uniaxial interface anisotropy is dominant.<sup>13</sup> The samples and measurement techniques are the same as those reported in Ref. 8. The experimental reversal time varied, depending on the thickness of the Fe film, from 1.6 to 2.5  $\mu$ s for a sinusoidal applied magnetic field of amplitude 120 Oe and frequency  $\Omega = 2500$  s<sup>-1</sup>. In Table I the results obtained with model 2 are shown. Similar times were obtained with model 1. The parameters introduced were approximately the ones experimentally found for  $\mu$  and  $\rho$  in Refs. 11 and 12 for Fe ultrathin films ( $\mu = 108$  (m/s)/Oe and  $\rho \approx 5 \times 10^{-6}$  m<sup>-2</sup>). The computed reversal times agree reasonably well with experimental results.

### D. Comparison between models

To see the difference in predicted behavior between models 1 (straight wall) and 2 (circular wall), Fig. 7(a) shows two hysteresis loops calculated with the same parameter values, using both models. During the first stages of the reversal, the

TABLE I. Reversal times computed with model 2, for different values of  $\mu$  and  $\rho$ .

	$\rho = 10^6 \text{ m}^{-2}$	$\rho = 10^7 \text{ m}^{-2}$
$\mu = 50 \frac{\text{m/s}}{\text{Oe}}$	$3.2 \mu\text{s}$	$1.8 \mu\text{s}$
$\mu = 100 \frac{\text{m/s}}{\text{Oe}}$	$2.2 \mu\text{s}$	$1.3 \mu\text{s}$
$\mu = 200 \frac{\text{m/s}}{\text{Oe}}$	$1.6 \mu\text{s}$	$1.0 \mu\text{s}$

process is faster in model 1 than 2, but as the radius of the circular domain wall increases, the reversal gets faster in model 2 since the reversal goes linearly with time in model 1 and as the square of time in model 2. A difference in the dependence of  $H_c^*$  on  $\ln(\Delta H/\Delta t)$  was also seen. Figure 7(b) shows this difference is not important.

Finally, in order to investigate the effect of nucleation, a nucleation rate  $\eta$  was considered in model 3. Figure 8 shows the results obtained: it lowers  $H_c^*$  at high sweep rates. Given a certain mobility ( $\mu$ ), more nucleation means quicker reversal and, consequently, lower  $H_c^*$ . That is, in this model, nucleation does not increase the slope of  $H_c^*$  vs  $\ln(\Delta H/\Delta t)$ , as suggested by other works,<sup>2</sup> but has the opposite effect.

## V. CONCLUSIONS

We have presented a model for dynamic reversal in ultrathin ferromagnetic layers. The model is based on the experimental findings that (i) the velocity of the domain wall within these systems responds linearly to the applied magnetic field following Eq. (1) (Ref. 11) and (ii) that these systems reverse via nucleation and propagation of quasircular domain walls.<sup>12</sup> Our model has two intrinsic parameters ( $h_{dp}$  and  $\mathcal{T} = \mu\sqrt{\rho}$ ) that correspond to characteristics of the samples (magnetocrystalline structure, thickness, and growth conditions).

Our model implies that, in a given sample, the reversal time will determine the frontier between the low dynamic and high dynamic regimes seen in experiments. When the period of the sinusoidal applied field ( $T$ ) is much higher than the reversal time (RT), a linear response is seen in the  $\ln(H_c^*)$  vs  $\ln(\Delta H/\Delta t)$  data. On the contrary, when  $T \sim \text{RT}$ , then the coercivity of the films increases rapidly. On the

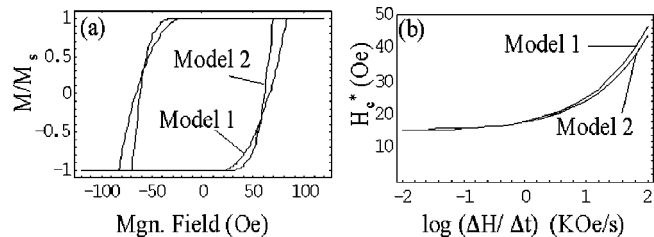


FIG. 7. Hysteresis loops (a) and dynamic coercive field (b), models 1 and 2,  $H_0 = 120 \text{ Oe}$ ,  $h_{dp} = 20 \text{ Oe}$ ,  $\Omega = 10^{5.5}$ ,  $\mu = 100 \text{ (m/s)/Oe}$ , and  $\rho = 10^6 \text{ m}^{-2}$ .

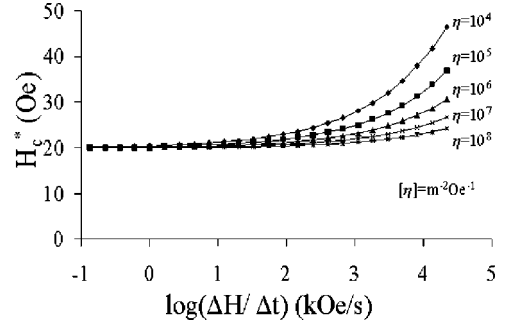


FIG. 8.  $H_c^*$  vs sweep rate.  $H_0 = 150 \text{ Oe}$ , and  $h_{dp} = 20 \text{ Oe}$ ,  $\mu = 100 \text{ (m/s)/Oe}$ , using model 3.

other hand, the role of  $h_{dp}$  is to shift the  $\ln(H_c^*)$  vs  $\ln(\Delta H/\Delta t)$  plot up (down) when it increases (decreases).

We have seen how using similar values both for  $\mu$  and for  $\rho$  to those experimentally obtained from Refs. 11 and 12, it has been possible to obtain the reversal time (Table I) of actual samples of epitaxial ultrathin Fe/GaAs(001) and Fe/InAs(001) films.<sup>8</sup> Also, it has been possible to match experimental data of  $\ln(H_c^*)$  vs  $\ln(\Delta H/\Delta t)$  without changing the parameters of the model for each sample.

Comparing the results of the calculations performed with experimental data, a correlation between  $\mathcal{T} = \mu\sqrt{\rho}$  and the thickness ( $t$ ) of the film has been found:  $t \approx a\mathcal{T}^b$ . Here  $a = 1.75$  and  $b = 0.43$  are the values found for the set of samples reported in Ref. 8. Qualitatively, this can be interpreted in terms of the importance of the roughness of the interfaces of the magnetic film both for domain wall pinning and nucleation of reversed domains. The thinner the film is, the more important the presence of roughness is expected to be since it will have a higher influence on the domain wall pinning and, perhaps, on the nucleation of reversed domains.

## ACKNOWLEDGMENTS

We would like to thank Dr. W. Y. Lee for technical support. I.R.-F. would like to thank S. Gardiner for helpful discussions and help in the computer implementation of the model. Also, the European Commission for financial support under the ESPRIT project MASSDOTS, No. 22464, under the Marie Curie Scheme, fourth framework program, Contract No. ERBFM-BICT983157, and fifth framework program, Contract No. HPMF-1999-00141.

## APPENDIX: COMPUTATIONAL DETAILS

The method used to compute hysteresis loops was as follows. The inputs of the program were  $H_0$  and  $\Omega$  for the applied field and  $h_{dp}$ ,  $\mu$ , and  $\rho$  for the sample parameters. Each loops was computed using  $N$  points (the data at each point  $i$  will be indicated with a subscript). Time was discretized with even intervals  $\Delta t = T/N$ , where  $T$  is the period of the sinusoidal applied field. The normalized magnetization ( $m$ ) was equal to  $-1$  at the beginning ( $m_1 = -1$ ). The magnetic field at each point was  $h_i = H_0 \sin(2\pi\Omega t_i)$ .

The calculation routine used in model 1 will now be briefly described. For each point, the magnetization was  $m_i = m_{i-1} + \Delta m_i$ . The value of  $\Delta m_i$  was determined by the first of the following choices that holds true for the point  $i$ :

- (i) If  $m_{i-1} = 1$  and  $h_i > h_{dp} \Rightarrow \Delta m_i = 0$ .
- (ii) If  $m_{i-1} = -1$  and  $h_i < -h_{dp} \Rightarrow \Delta m_i = 0$ .
- (iii) If  $h_i \geq 0 \Rightarrow$  the evolution equation (4) was used.

(iv) If  $h_i < 0 \Rightarrow$  the evolution equation (4) was used.

In the third and fourth cases, if  $m_{i-1} + \Delta m_i$  exceeded 1 or  $-1$ , respectively, then saturation was reached, and  $m_i = 1$  or  $-1$ , respectively, was imposed.

This routine was used in model 1. For model 2, eight cases, instead of four, were necessary to cover all the possibilities, and 16 cases were necessary for model 3.

<sup>1</sup>W. Y. Lee, Y. B. Xu, S. M. Gardiner, and J. A. C. Bland, *J. Appl. Phys.* **87**, 5926 (2000).

<sup>2</sup>B. Raquet, R. Mamy, and J. C. Ousset, *Phys. Rev. B* **54**, 4128 (1996).

<sup>3</sup>W. Y. Lee, B.-Ch. Choi, Y. B. Xu, and J. A. C. Bland, *Phys. Rev. B* **60**, 10 216 (1999).

<sup>4</sup>Y.-L. He and G.-C. Wang, *Phys. Rev. Lett.* **70**, 2336 (1993).

<sup>5</sup>Q. Jiang, H.-N. Yang, and G.-C. Wang, *Phys. Rev. B* **52**, 14 911 (1995).

<sup>6</sup>J.-S. Suen and J. L. Erskine, *Phys. Rev. Lett.* **78**, 3567 (1997).

<sup>7</sup>J.-S. Suen, M. H. Lee, G. Teeter, and J. L. Erskine, *Phys. Rev. B* **59**, 4249 (1999).

<sup>8</sup>T. A. Moore, J. Rothman, Y. B. Xu, and J. A. C. Bland, *J. Appl.*

*Phys.* **89**, 7018 (2001).

<sup>9</sup>M. P. Sharrock and J. T. McKinney, *IEEE Trans. Magn.* **MAG-17**, 3020 (1981).

<sup>10</sup>P. Bruno, G. Bayreuther, P. Beauvillain, C. Chappert, G. Lugert, D. Renard, J. P. Renard, and J. Seiden, *J. Appl. Phys.* **68**, 5759 (1990).

<sup>11</sup>R. P. Cowburn, J. Ferre, S. J. Gray, and J. A. C. Bland, *Appl. Phys. Lett.* **74**, 1018 (1999).

<sup>12</sup>R. P. Cowburn, J. Ferre, S. J. Gray, and J. A. C. Bland, *Phys. Rev. B* **58**, 11 507 (1998).

<sup>13</sup>Y. B. Xu, D. J. Freeland, M. Tselepi, and J. A. C. Bland, *J. Appl. Phys.* **87**, 6110 (2000).